Contribution of an accurate growth rate reconstruction of a stalagmite from the Kanaan Cave-Lebanon to the understanding of humidity variations in the Levant during the MIS 5

Carole Nehme[1,2,*], Sophie Verheyden[1], Stephen Noble[3], Andrew Farrant[4], Jean-Jacques Delannoy[2]

[1] Department of Earth and History of Life. Royal Institute of Natural Sciences (RBINS), Brussels, Belgium.
[2] EDYTEM UMR 5204-CNRS, Université de Savoie, le Bourget du Lac, France.
[3] NERC Isotope Geochemistry Laboratory, British Geological Survey, Keyworth, United Kingdom.
[4] British Geological Survey, Keyworth, United Kingdom.
* corresponding author: cnehme@naturalsciences.be

ABSTRACT. Lying at the transition between temperate Mediterranean domain and subtropical deserts, the Levant is a key area to study the palaeoclimatic response over glacial-interglacial cycles. This paper presents a dated last interglacial (MIS 5) stalagmite (129–84 ka) from the Kanaan Cave, Lebanon. Variations in growth rate, morphology and petrology have been measured to derive a palaeoclimatic record. The speleothem growth curve shows rapid growth rates during the peak of MIS 5e (126-124 ka), moderate growth rates between 103.5 and 99 ka and very low growth rates from 99 to 84 ka. On the basis of the good correlation between the speleothem morphology and growth rates with the isotopic response of continental records from northern and southern Levant, we relate high growth rate to wet conditions during the maximum MIS 5e and MIS 5c. The peak in growth rates corresponds to sapropel events in the eastern Mediterranean. Low growth rates during MIS 5d and 5b indicate a transition to drier conditions.

KEYWORDS: Palaeoclimate, MIS 5, Lebanon, stalagmite, growth rate, Kanaan cave

1. Introduction

Located at the interface between mid and high latitude climate systems, and affected by both the North Atlantic Oscillation and the monsoonal system over Africa, the Levant region (East Mediterranean Basin) has the unique potential to record the occurrence and phasing of climatic changes in both systems. Known for its long records of prehistoric human settlements, the Levant straddles the transition zone between the humid Mediterranean climate in the north and the arid Saharo-Arabian desert climate in the south. This transition zone is characterised by steep precipitation and temperature gradients. Over the past decade, several studies have attempted to understand the palaeoclimate of this critical region (Fig. 1a) using both marine (Rossignol-Strick, 1999; Kallel et al., 1997; Emeis et al., 2003) and continental palaeoclimate records (Frumkin et al., 2000; Bar-Mathews et al., 2003; Ayalon et al., 2013; Vaks et al., 2010; Kolodny et al., 2005; Gasse et al., 2011, 2015; Develle et al., 2011). A key period for understanding the climate system in the Levant is the last interglacial. This is generally considered to be a warm period, comparable to the present-day climate, although this is still under considerable debate. Discrepancies between different palaeoclimate archives exist, particularly between speleothem and lacustrine archives. In particular, inconsistencies between records from Negev desert (Vaks et al., 2010), central Palestine/Israel (Bar-Mathews et al., 2000; 2003; Frumkin et al., 2000) and northern Levant (Develle et al., 2011; Gasse et al., 2011; 2015), and between the eastern Mediterranean coastline (Ayalon et al., 2013) and inner basins (i.e. Dead Sea Basin) (Kolodny et al., 2005; Waldmann et al., 2009) are evident. One of the main inconsistencies is the wet phases demonstrated from speleothem isotopic records of Soreq, Peqiin and West Jerusalem caves, during the interglacial optimum and the dry phases shown from the low lake levels in the Dead Sea basin.

Whereas these different continental records reflect changes in atmospheric circulation, regional topographic patterns and/or site-specific climatic and hydrological factors, the lack of long-term records from the northern Levant, especially from different continental archives, limits our understanding of the regional response to climatic conditions during Marine Isotope Stage (MIS) 5. This lack of data restricts the opportunities to resolve the inconsistencies between palaeoclimate records across the region. This study attempts to resolve this by providing a new high-resolution record obtained from a speleothem from a cave situated on the west flank of Mount Lebanon. Speleothems are secondary chemical cave deposits, which provide high-resolution proxy tools for palaeoclimate reconstruction (Genty et al., 2001;

Verheyden, 2001; Verheyden et al., 2006). Recent studies highlight the significance of speleothem records, in particular for achieving precise chronologies of continental climate changes (Wang et al., 2001; Fairchild et al., 2006; Genty et al., 2003, 2006).

A stalagmite from Kanaan Cave in central Lebanon is dated and climate indicators (growth phases, growth rate and petrographic characteristics) investigated as a first attempt to document the regional climate change during the last interglacial in the northern Levant. This study also highlights the influence of speleogenetic factors within Kanaan Cave on speleothem deposition.

2. Climate and palaeoclimate settings

Lebanon is located along the central-eastern coastline of the Mediterranean Sea between latitudes 32°34′N and 34°41′N (Fig. 1a). The western side of Mount Lebanon is characterized by a Mediterranean climate with an annual precipitation varying between 880 and 1100 mm along the coastline (World Bank, 2003). The climate is seasonal, with rainy winters (between November and February) and dry, hot summers (from May to October).

Speleothem records, among other palaeoclimatic proxies, have contributed to the reconstruction of the MIS 5 climate in the Levant region (Frumkin et al., 1999; 2000; Bar-Mathews et al., 1999; 2000; 2003; Ayalon et al., 2013, Vaks et al., 2006; 2010). These climate characteristics are highlighted below and summarized in Table 1. Just after the end of the Termination II (~140-130 ka) during which time the climate was generally wet and cold, the region experienced an intense warm period coinciding with the development of anoxic conditions (Sapropel 5) in the Eastern Mediterranean (Rossignol-Strick, 1999; Emeis et al., 2003) and maximum northern hemisphere summer insolation (Berger & Loutre, 1991). From ~130-120 ka, speleothems records from Peqiin, Soreq and West Jerusalem record periods of rapid growth, mainly attributed to higher rainfall (Bar-Mathews et al., 2003), suggesting conditions were wetter than the Holocene period. Corresponding high $\delta^{13}C$ records were interpreted as a consequence of soil denudation with high surface runoff (Bar-Mathews et al., 2003) or due to intense forest fires (Frumkin et al., 2000). Wet conditions (~125-117 ka) are suggested also by other proxies, such as pollen and oxygen lake isotopes derived from ostracods shells, from the northern Levant (Gasse et al., 2011; 2015). However, the Dead Sea Basin remained dry at this time (Kolodny et al., 2005) and Samra lake levels were lower than the Holocene, even though a slight rise occurred (Waldmann et al., 2009) during the late Interglacial Maximum.

MIS	MIS 5a	MIS 5b	MIS 5c	MIS 5d	MIS 5e	MIS 6.2- Terminaison II
Ages	75 - 85 ka	85-100 ka	100-108 ka	108-118 ka	118-128 ka	130-140 ka
N. Hemisphere summer/winter Insolation	- Max June Insolation: ~520 W/m^2		- Max winter Insolation: ~240 W/m^2		- Max June Insolation: ~535 W/m^2	
EM Basin	- Anoxic conditions S3 - SST ~ 17.9 °C - Low surface salinity. δ_w ~ +0.5‰	- SST ~ 14.5 °C	- Anoxic conditions S4 - SST ~ 18.5 °C - Low surface salinity. δ_w ~ 0‰	- SST ~ 20.4 °C	- Anoxic conditions S5 - SST ~ 20.5 °C - Low surface salinity. δ_w ~ -0.3‰	- SST ~ 13.8 °C
N. Levant Yammouneh Paleolake	- *Quercus/ Artemisia/ Chenopidiaceae* Carbonate enrichment	- Pines/open vegetation	- *Quercus/ Artemisia/ Chenopidiaceae* Carbonate enrichment	- Evergreen oaks/pines	- Oaks forests Sharp carbonate enrichment	- Junipers
S. Levant W Jerusalem Cave	- Increased C3 vegetation	- Increased C3 vegetation	- Increased C3 vegetation	- Increasing proportion of C3 vegetation	- Soil coverage loss and/or vegetation of high C3/C4 ratio	- Dense C3 vegetation
Soreq & Peqiin Caves	O^{18}-depleted values (-5.8 to -7‰)	O^{18}-enriched values (-4 to -5‰)	O^{18}-depleted values (-5 to -7.8‰)	O^{18}-enriched values (-3.8 to -5.2‰)	O^{18}-depleted values (-6.5 to -8.7‰)	O^{18}-enriched values (-2.6 to -3.8‰)
Dead Sea Basin (DSB)	- Very low lake levels	- Higher lake-levels	- Low lake levels	- Lake-level decline	- Slight rise in lake level (~60 m)	- Very low lake levels
S. Negev			Speleothem deposition NHP-1	Speleothem deposition NHP-1	Speleothem deposition NHP-1	

Table 1. Summary of previous studies presenting the palaeoclimatic conditions prevailing in the Levant region during MIS 5: Northern Insolation (Berger & Loutre, 1991), East Mediterranean Sea (Rossignol-Strick, 1999; Emeis et al., 2003), Yammouneh Paleolake in northern Lebanon (Develle et al., 2011; Gasse et al., 2011; 2015), West Jerusalem, Soreq and Peqiin Caves (Frumkin et al., 2000; Bar-Mathews et al., 2000; 2003), Dead Sea Basin (Kolodny et al., 2005; Waldmann et al., 2009; Lisker et al., 2010), and Tzavoa Cave, Negev (Vaks et al., 2006; 2010).

Sample Number	Distance from base (cm)	U (ppm)	^{232}Th (ppb)	[^{230}Th/^{232}Th] (measured)	[^{230}Th/^{238}U] (corrected)	[^{234}U/^{238}U] (corrected)	$\rho_{08\text{-}48}$	Age uncorrected (ka)	Age corrected (ka)	Age BP$_{1950}$ corrected (ka)	[^{234}U/^{238}U]$_{initial}$
KA STM 1-4	**2.4**	0.1549	0.5079	520.1	0.5602 ± 0.27	0.8328 ± 0.13	0.07	129.92 ± 0.80	**129.79 ± 0.80**	**129.72 ± 0.80**	0.7588 ± 0.26
KA STM 1-5	**2.9**	0.1425	1.623	147.2	0.5497 ± 0.37	0.8297 ± 0.18	0.47	126.47 ± 0.77	**126.02 ± 0.83**	**125.96 ± 0.83**	0.7570 ± 0.26
KA STM 1-6	**4.1**	0.07508	3.488	37.5	0.5665 ± 1.0	0.8298 ± 0.56	0.85	135.85 ± 0.97	**133.99 ± 1.63**	**133.93 ± 1.63**	0.7515 ± 0.93
KA STM 1-7	**5.2**	0.05155	1.207	74.1	0.5671 ± 0.59	0.8558 ± 0.31	0.67	125.46 ± 0.89	**124.57 ± 1.08**	**124.51 ± 1.08**	0.7950 ± 0.50
KA STM 1-8	**6.9**	0.05426	2.676	35.1	0.5623 ± 1.1	0.8640 ± 0.59	0.82	121.74 ± 0.82	**119.91 ± 1.53**	**119.84 ± 1.53**	0.8092 ± 0.87
KA STM 1-9	**7.9**	0.07067	0.8548	139.8	0.5541 ± 0.40	0.8809 ± 0.19	0.42	112.31 ± 0.68	**111.88 ± 0.74**	**111.81 ± 0.74**	0.8367 ± 0.24
KA STM 1-2	**8.8**	0.06580	0.8400	124.6	0.5208 ± 0.51	0.8716 ± 0.31	0.26	103.03 ± 0.90	**102.57 ± 0.96**	**102.50 ± 0.96**	0.8284 ± 0.48
KA STM 1-10	**11.6**	0.05592	0.7053	121.9	0.5037 ± 0.45	0.8579 ± 0.21	0.44	100.41 ± 0.61	**99.94 ± 0.69**	**99.88 ± 0.69**	0.8116 ± 0.25
KA STM 1-11	**13.5**	0.07340	0.2089	516.7	0.4829 ± 0.30	0.8532 ± 0.13	0.06	94.27 ± 0.50	**94.16 ± 0.51**	**94.10 ± 0.51**	0.8085 ± 0.25
KA STM 1-3	**19.5**	0.05971	0.7545	108.5	0.4486 ± 0.56	0.8439 ± 0.33	0.27	85.83 ± 0.70	**85.36 ± 0.78**	**85.30 ± 0.78**	0.8014 ± 0.50

Table 2. Uranium series dating results of K1-2010 stalagmite.
All uncertainties are ±2σ. ^{230}Th and ^{234}U decay constants are from Cheng et al., 2013, ^{238}U decay constant from Jaffey et al., 1971. Detrital Th corrections assumed an initial ^{230}Th/^{232}Th atomic ratio = 4.4 x 10^{-6} ± 50% and bulk earth ^{232}Th/^{238}U = 3.8.

Between ~118 and ~110 ka, a return to slightly drier conditions is suggested by an increase in $\delta^{13}C$ values and $\delta^{18}O$ enrichment obtained from speleothem data in southern Levant, suggesting lower rainfall amounts. However evidence for C3 vegetation cover, indicative of wet conditions, is suggested in West Jerusalem Cave (Frumkin et al., 2000), whilst the Yammouneh palaeolake record in the northern Levant (Develle et al., 2011) suggests seasonal changes with wet winters and dry summers.

From ~110 to ~100 ka, a short wet period is observed from depleted $\delta^{18}O$ values in speleothem from the southern Levant and from arboreal pollen taxa in the northern Lebanon (Develle et al., 2011). This coincides with anoxic conditions (Sapropel 4) in the eastern Mediterranean (Emeis et al., 2003). Between ~100 and ~85 ka, a return to a colder climate is suggested by speleothem deposition in Soreq, Peqiin and West Jerusalem with $\delta^{18}O$-enriched values. However, the C3 vegetation cover persisted in the southern Levant (Frumkin et al., 2000) and a slight lake level increase in the Dead Sea Basin occurred (Waldmann et al., 2009).

From ~85.0 to ~75.0 ka, the last wet and warming phase of MIS 5 occurred in the Levant, corresponding with the Sapropel (S3) formation in eastern Mediterranean and with the maximum northern hemisphere insolation (65°N July) (Berger & Loutre, 1991). In western Palestine/Israel, depleted $\delta^{18}O$ values from speleothems in the Soreq, Peqiin (Bar-Mathews et al., 1999; 2003) and Ma'aele Effrayim caves (Ayalon et al., 2013) as well as an increase in arboreal pollen taxa in the Yammouneh lacustrine record (Develle et al., 2011) suggest a moderate wet period at this time. However, the level of Lake Lisan in the Dead Sea Basin decreased significantly (Waldmann et al., 2009) and no speleothem deposition occurred after the MIS 5c in Southern Negev (Vaks et al., 2006; 2010), both suggesting a drier climate during MIS 5a in the south of the region.

3. Location of Kanaan Cave

Mount Lebanon consists mainly of carbonate rocks of Jurassic to Cretaceous age. Within these carbonates are numerous caves with an abundance of well-preserved speleothem deposits. Kanaan Cave is located within the western flank of central Mount Lebanon. The entrance of the cave is located in the southern side of the Antelias river valley at N 33°54′25″; E 35°36′25″ at 98 m above sea level (a.s.l.). It is located ~2 km east of the Mediterranean coast and ~10 km north of Beirut. The cave system is entirely developed in the Middle Jurassic Kesrouane Formation, a thick sequence of predominantly micritic limestone and dolomite, which has an average stratigraphic thickness of 1000 m (Fig. 1b).

The Kanaan Cave is a relict conduit and now perched 65 m above the active hydrological network draining to springs lower down the Antelias valley. The cave entrance was discovered during quarrying in 1997. Various studies have been undertaken in the cave including petrographic analysis of speleothems (Nader, 1998), speleogenetic and palaeogeographical reconstructions (Nehme et al., 2009), and seismic hazard analysis (Lacave et al., 2012). The cave is 162 m long and divided into three main parts: i) the Entrance Gallery showing fallen fragments of calcite drapery and flowstone; ii) two collapse chambers (named Collapse I and II) with fallen blocks resting over clay sediment; iii) the Corridor Gallery in the inner part of the cave, partially filled by clay deposits and covered by various speleothem deposits (flowstone, stalagmites, stalactites). The present end of the cave is blocked by massive speleothem.

The stalagmite K1-2010 was collected from on top of a fallen block of limestone in the center part of the Collapse I chamber, ~20 m from the cave entrance (Fig. 1c). Whilst currently near the entrance, the cave was sealed prior to quarrying in 1997. The ceiling of the cave at this location is 2.4 m high, and the thickness of the limestone overburden is ~50 m. Presently the stalagmite receives no dripping water, although some drip water occurs in other parts of the Collapse I chamber during winter and spring seasons. The cave is generally dry during the summer months. The air temperature in Collapse I chamber is ~20 °C.

4. Methods

The stalagmite was cut along its growth axis after retrieval from the cave. The investigated section was polished using 120 - 4000 μm silicon carbide (SiC) paper. Crystallographic observations were performed with an optical binocular microscope NEOC.

Uranium series speleothem dating was carried out at the NERC Isotope Geosciences Laboratory (NIGL), British Geological Survey, Keyworth, UK. Powdered 100 to 400 mg calcite samples were collected with a dental drill from ten locations along the growth axis of the speleothem, taking care to sample along growth horizons. Chemical separation and purification of uranium and thorium were performed following the procedures of Edwards et al. (1987) and Anderson et al. (2008). Uranium series age data were obtained on a Thermo Triton thermal ionization mass spectrometer (TIMS) employing a Mascom SEM and RPQ and following procedures modified from Anderson et al. (2008) and Hiess et al. (2012). Mass bias and SEM gain for Th measurements were corrected using an in-house ^{229}Th–^{230}Th–^{232}Th reference solution calibrated by ICP-MS against CRM 112a. Quoted
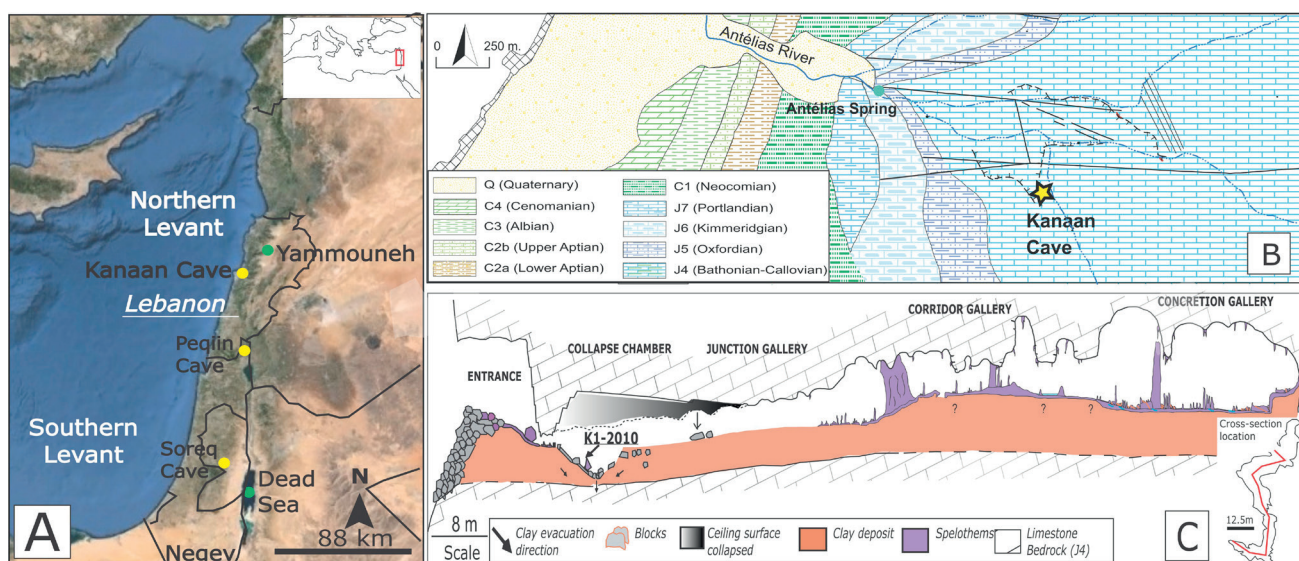
Figure 1. (A) Location map of Kanaan cave and the continental records in the Levant. (B) Geological map of the Antelias region (western flank of central Mount-Lebanon) (Dubertret, 1975). (C) Geomorphological section of Kanaan Cave showing the location of the stalagmite K1-2010 in the Collapse Chamber (Nehme, 2013).

uncertainties for activity ratios, initial $^{234}U/^{238}U$, and ages include a ca. 0.2% uncertainty calculated from the combined $^{236}U/^{229}Th$ tracer calibration uncertainty and measurement reproducibility of reference materials (HU-1, CRM 112a, in-house Th reference solution) as well as the measured isotope ratio uncertainty. All ages are given in years before BP 1950 with an uncertainty at the 2σ level, typically of between 500 and 1000 years.

5. Results

5.1. Petrography

The K1-2010 stalagmite is 23 cm long and up to 10 cm wide (Fig. 2). The longitudinal inner profile of the stalagmite displays a regular deposition of dense calcite ranging in colour from dark brown to light yellow with a regular thin lamination (< 0.2 mm) at certain parts. At the lower and upper parts of the stalagmite, the calcite is denser and mainly displays uniform yellow translucent texture. The stalagmite is divided into two main segments.

The lower segment (segment 1) is 8.2 cm long and 8.5 cm wide and displays a general growth axis tilted at a 45° angle (clockwise) relative to the upper part of the speleothem. Between 8.2 and 2.6 cm from the base of the segment 1 (Fig. 2), a regular deposition of translucent columnar crystals prevailed, locally interrupted by marked dark brown layers (discontinuities) at 5.9 cm and from 3.3 to 3.6 cm. Between 0 and 2.6 cm, a continuous layering prevailed with a clear and translucent texture in the central part of the laminas (apex) and turning to a dark brown colour at the border.

The higher segment (segment 2) is 12.3 cm long and 4-6 cm wide (Fig. 2), and displays a general growth axis tilted at 16° (counter clockwise) to the vertical at the base, gradually becoming more vertical towards the top. The general structure of this section is characterised by uniform yellow translucent columnar crystals interrupted by a marked opaque yellow layers, respectively at 9, 8, 5.6, 3.2 and 2.8 cm from the base of the segment 2.

5.2. Uranium series (U/Th) dating

Ten uranium series dates obtained from regular intervals along the growth axis of the speleothem (Table 2) indicates that the stalagmite K1-2010 was deposited approximately from 129.72 $\pm$ 0.8 (2σ) ka to 85.3 $\pm$ 0.7 ka. The measured uncertainties are greatest in the lower part (Segment 2) of the speleothem where detrital layers prevail. The dates are in stratigraphic order with the exception of sample KA-8. This is possibly due to the presence of detrital matter in the laminas. This sample also has the largest error bars.

6. Discussion

6.1. Growth curve description

Growth of speleothems is generally conditioned by effective precipitation and CO_2 concentration, controlled mainly by a developed bio-activity of the soil and consequently by the temperature (Baker & Smart, 1995; Dreybrodt, 1988; Genty et al., 2006). In the Levant, higher speleothem growth rates could be associated with warm conditions and higher water availability whereas low speleothem growth rates could indicate cold or dry conditions.

An age versus depth profile for the K1-2010 stalagmite was derived from the ten uranium series dates, which suggest
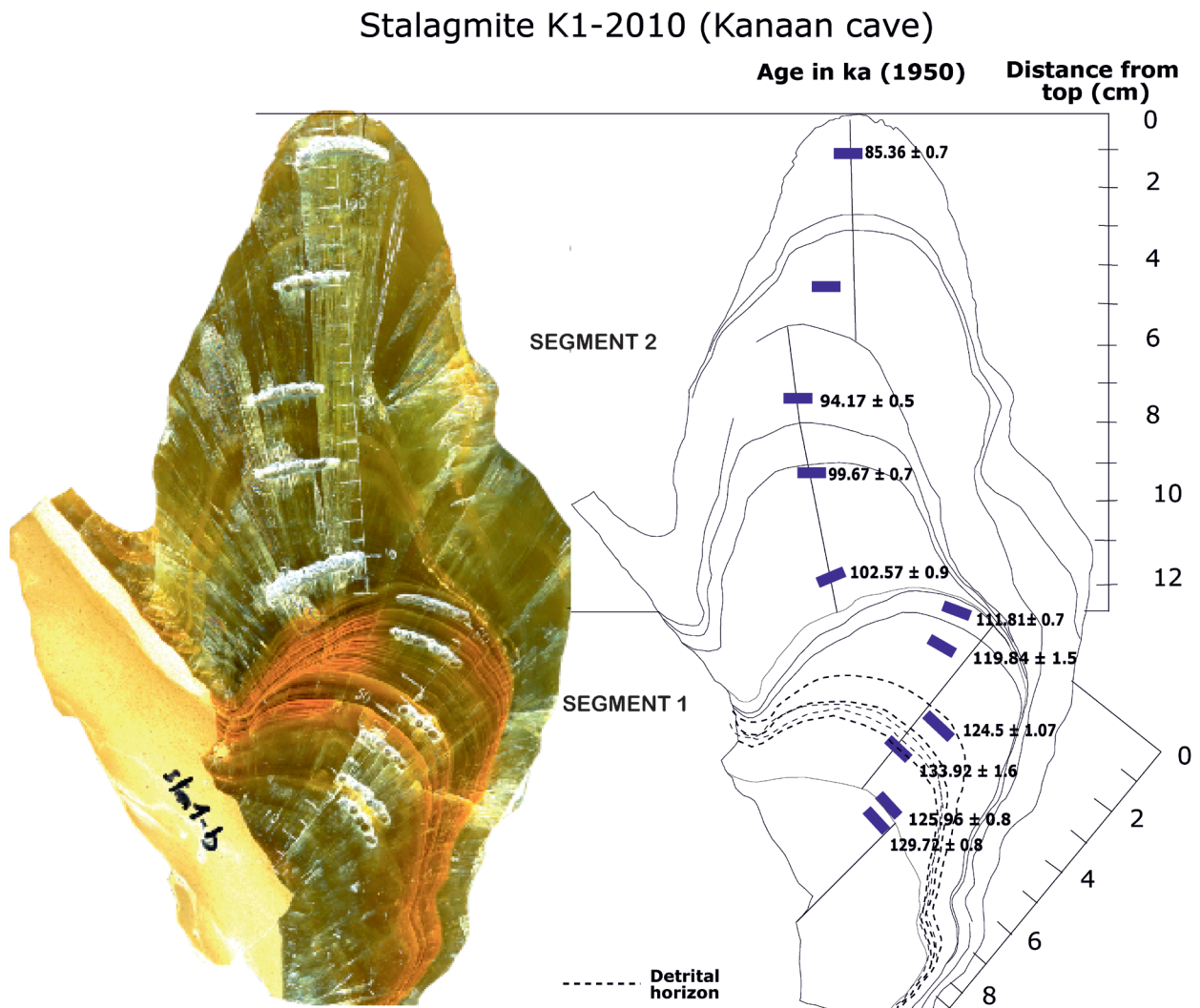
Figure 2. Cut face of the K1-2010 speleothem and a sketch showing the Uranium series age data.

Figure 3. Growth rate of the stalagmite with respect to distance (in mm) from the top, assuming linear growth rates between two consecutive dates except in the middle part where a discontinuity (hiatus) is identified. S5, S4 and S3 are the sapropel events in the Eastern Mediterranean basin from ~128-122 ka, ~110-100 ka and ~85-75 ka respectively (Ziegler et al., 2010) during which enhanced rainfall events occurred over the Eastern Mediterranean region (Bar-Mathews et al., 2003).
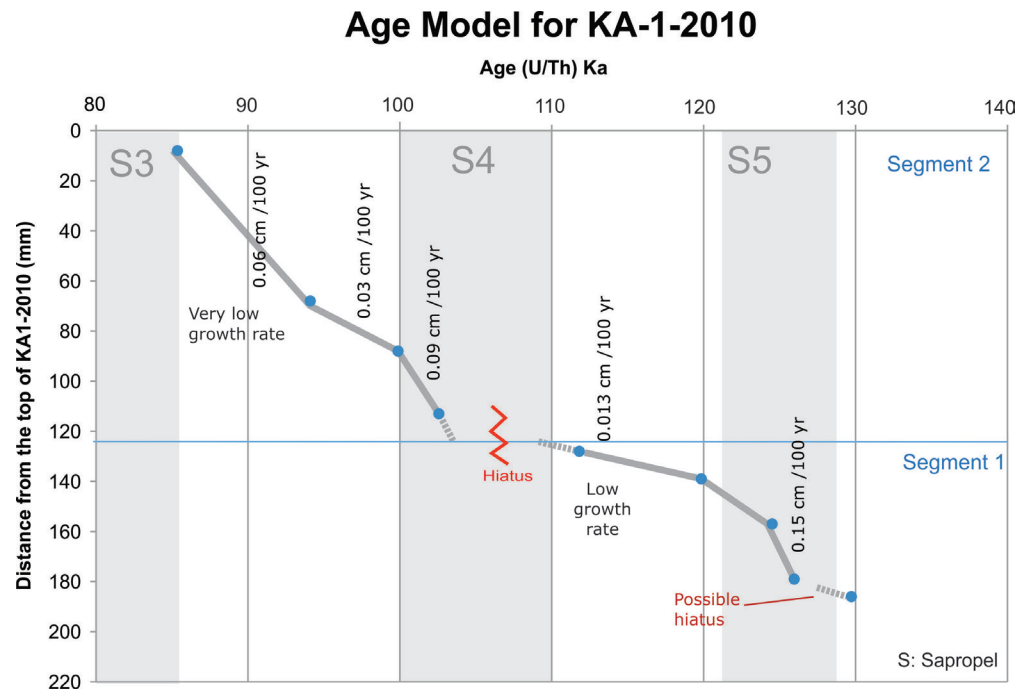
growth rates varied from 0.013 to 0.15 cm/100a (Fig. 3). The highest growth rate are between 124.45 ± 1 and 125.9 ± 0.8 (0.15 cm/100a) and between ~109 ka (extrapolated) and 99.8 ± 0.7 ka (0.09 cm/100a) and coincide with the maximum diameter in both segments 1 and 2. Very low growth rates (0.03 to 0.06 cm/100a) are measured between 99.8 ± 0.7 ka to 85.3 ± 0.8 ka and correspond to the smallest diameter. The lowest growth rate measured is between 119.84 ± 1.5 ka and 111.75 ± 0.74 ka (0.013 cm/100a). The higher segment grew continuously from 102.5 ± 0.96 to 85.3 ± 0.8 ka without any hiatuses. Several discontinuities were noted in the middle and the lower part, which precluded the extrapolation of a basal age for the stalagmite. An extrapolated age of 84.1 ka for the top of the stalagmite was estimated from the age model. The discontinuity in the middle part (Fig. 3) lasted from 109 to 103.5 ka (extrapolated) during which the growth axis was tilted by about 45°. However a possible discontinuity lasted from ~129 to ~126 ka in the lower segment and correspond to local factors that prevented the stalagmite from growing.

6.2. Speleogenetic context of the stalagmite growth in Kanaan Cave

The stalagmite K1-2010 initiated after the cave was disconnected from the active drainage system and following a period of roof collapse and sedimentation. The present irregular broken floor of the Collapse Chambers, largely consisting of breakdown blocks and speleothem, is due to the removal of sediment underlying the cave floor, causing the floor to subside (Nehme et al., 2013). Suffosion process, which is still on-going presently in the cave, is mainly the consequence of enlarged fissures under the cave level and subsequent to the migration of the water table downstream of Antelias karst system. The fissure enlargement is conditioned by continuous infiltration of aggressive water influx that triggers physico-chemical reactions (Ford & Williams, 2007) leading to limestone corrosion and subsequently clay withdrawal and floor subsidence in Kanaan cave. This continuous process triggered several mechanisms that influenced K1-2010 stalagmite growth during the MIS 5. The detrital layer (Fig. 2) between ~129 and ~126 ka indicates a possible discontinuity related to mud deposition over the stalagmite. The reconstitution of the tilted axe in segment 2, that grew over a breakdown block, showed that the stalagmite grew vertically over an already subsided floor on which the breakdown block was leaned about 15 to 20° (Nehme et al., 2013). This topographical configuration was sufficient to drain infiltrated water in the Collapse Chamber and cause ponding in this area and during which muddy water covered the stalagmite and prevented it from growing. Clay layers are observed on the outer edge of several growth laminae after ~126 ka, whereas the

apex remained relatively clean. These clay laminae suggest that the ponding process was still active until ~120 ka and less intense until ~111 ka but without preventing calcite deposition. This may have been more likely a consequence of increased water infiltration through the vadose zone during this period.

Between ~109 to ~103.5 ka, sediment evacuation continued beneath the cave floor leading to a consequent subsidence in the Collapse Chamber and thus tilting the speleothem by around 45°. Continued minor movement occurred during the deposition of the upper segment, causing minor tilting of the growth axis. The absence of thin clay particles in the upper segment (segment 1) suggests that no water accumulation occurred in the collapse chamber after ~103.5 ka, probably due to the continuous clay evacuation with more enlarged fissures underneath the chamber floor, allowing water to drain away rapidly without leading to a ponding process.

6.3. Wet periods during the MIS 5 in the Levant

The K1-2010 stalagmite shows the highest growth rate between ~126 and ~124 ka, suggesting that this was the wettest phase of MIS 5e in Lebanon. This coincides well with pollen and oxygen isotope records from the Yammouneh palaeolake (Gasse et al., 2011; Develle et al., 2011) at 1350 m a.s.l. Arboral taxa (*Quercus*) concentrated within the Yammouneh lake basin between ~125 and 117 ka suggest the climate was wet at this time. The speleothem growth rate reached its minimum (Fig. 3) after ~120 ka and continued at a low rate until 109 ka (extrapolated). A second wet phase from ~103.5 to ~99 ka occurred with a moderate growth rate, which corresponds to the wet phase suggested from the Yammouneh record between ~105 and ~100 ka (Develle et al., 2011). A return to colder, drier conditions is observed with the lowest growth rates between ~99 to ~84 ka. The speleothem record from Kanaan cave suggests that highest growth rates periods took place during sapropel events (Emeis et al., 2003) in the Eastern Mediterranean basin.

The sapropels are considered to have formed at times of enhanced low-latitude hydrological activity, mainly during marine isotope interglacial, but also during marine isotope glacial intervals. They correspond closely with the minima in the precession cycle (Lourens et al., 1996) when the East Mediterranean region experienced pluvial conditions (Cheddadi & Rossignol-Strick, 1995). The Mediterranean experienced strong salinity gradients due to also other processes occurring during sapropel events, such as meltwater discharge from the Euoroasian continental ice sheet or enhanced Nile discharge. However, the Mediterranean sea salinity depletion was associated

with enhanced rainfall throughout the Mediterranean basin (Kallel et al., 1997) because the S5 sapropels (Rossignol-Strick, 1999) developed after deglaciation, and therefore meltwater discharge could account less for their formation. Pollen assemblages found within sapropels S5 from the northeastern Mediterranean basin (Cheddadi & Rossignol-Strick, 1995) also support wet conditions.

Continental archives from the southern Levant, specifically speleothem isotopic records from Soreq, Peqiin and West Jerusalem caves (Bar-Mathews et al., 1999; 2003; Frumkin et al., 2000), show $\delta^{18}O$ depleted values during the MIS 5e and were linked to enhanced rainfall over the East Mediterranean basin. Higher growth rates from K1-2010 stalagmite, from Kanaan cave, Lebanon coincide with wet periods suggested from Yammouneh records, in northern Lebanon (Develle et al., 2011) and from Peqiin, West Jerusalem and Soreq caves in southern Levant during sapropel events.

Conversely, the Dead Sea Basin (DSB) conditions remained generally dry and palaeolake Samra experienced lowstands levels during the whole MIS 5 (Waldmann et al., 2009). In the southern Negev desert, speleothem and travertine deposition occurred, until MIS 5d (Vaks et al., 2010). These wet pulses were possibly associated with intrusions of humidity from southern sources during interglacial periods (Waldmann et al., 2009).

7. Conclusion

A dated MIS 5 stalagmite record (129–84 ka) from Kanaan Cave, Lebanon demonstrates the potential of stalagmite records for palaeoclimate reconstruction in the northern Levant. The age model of stalagmite K1-2010, derived from uranium series dating, coupled with the petrography analyses demonstrate high growth rates during MIS 5e, moderate growth rates during the MIS 5c and the lowest growth rates during the ensuing interstadial period MIS 5b. High and moderate growth rates corresponding with zones of maximum speleothem width are interpreted as the result of warm, moist periods and a higher water availability whereas the lowest growth rates resulted from colder, drier phases and less water availability in the vadose zone.

Clay layers incorporated between growth laminae during speleothem deposition in MIS 5e are attributed to higher water availability within the cave. The absence of detrital layers in the higher segment during MIS 5c and 5b is the result of less water flooding in the cave, possibly due to more local effects related to the subsidence of the cave floor, or possibly due to regional climatic effects.

K1-2010 growth rates results suggest wet and dry periods that are in agreement with pollen and stable isotopes proxies from Yammouneh lacustrine records in the northern Levant and from speleothems records of Peqiin, Soreq and West Jerusalem caves in the southern Levant. However, further stable isotopes analyses on K1-2010 are required in order to provide a more detailed, robust palaeoclimate record of MIS 5 in the northern Levant.

8. Acknowledgement

9. References

Andersen, M.B., Stirling, C.H., Potter, E.K., Halliday, A.N., Blake, S.G., McCulloch, M.T., Ayling, B.F. & O'Leary, M., 2008. High-precision U-series measurements of more than 500,000 year old fossil corals. Earth and Planetary Science Letters, 265, 229-245.

Ayalon, A., Bar-Matthews, M., Frumkin, A. & Matthews, A., 2013. Last Glacial warm events on Mount Hermon: the southern extension of the Alpine karst range in the east Mediterranean. Quaternary Science Reviews, 59, 43-56.

Baker, A. & Smart, P.L., 1995. Recent flowstone growth rates: field measurements in comparison to theoretical predictions. Chemical Geology, 122, 121-128.

Bar-Matthews, M., Ayalon, A., Kaufman, A. & Wasserburg, G.J., 1999. The Eastern Mediterranean paleoclimate as a reflection of regional events: Soreq Cave, Israel. Earth and Planetary Science Letters, 166, 85-95.

Bar-Matthews, M., Ayalon, A. & Kaufman, A., 2000. Timing and hydrological conditions of Sapropel events in the Eastern Mediterranean, as evident from speleothems, Soreq Cave, Israel. Chemical Geology, 169, 145-156.

Bar-Matthews, M., Ayalon, A., Gilmour, M., Matthews, M. & Hawkesworth, C., 2003. Sea-land isotopic relationships from planktonic foraminifera and speleothems in the Eastern Mediterranean region and their implications for paleorainfall during interglacial intervals. Geochimica et Cosmochimica Acta, 67, 3181-3199.

Berger, A. & Loutre, M.F., 1991. Insolation values for the climate of the last 10 million years. Quaternary Science Reviews, 10, 297-317.

Cheddadi, R. & Rossignol-Strick, M., 1995. Eastern Mediterranean Quaternary paleoclimates from pollen and isotope records of marine cores in the Nile cone area. Paleoceanography, 10, 291-300.

Cheng, H., Edwards, R.L., Shen, C.C., Polyak, V.J., Asmerom, Y., Woodhead, J., Hellstrom, J., Wang, Y., Kong, X., Spötl, C., Wang, X., Alexander Jr., E. Calvin, 2013. Improvements in ^{230}Th dating, ^{230}Th and ^{234}U half-life values, and U-Th isotopic measurements by multi-collector inductively coupled plasma mass spectrometry. Earth and Planetary Science Letters, 371-372, 82-91.

Develle, A.L., Gasse, F., Vidal, L., Williamson, D., Demory, F., Van Campo, E., Ghaleb, B. & Thouveny, N., 2011. A 250 ka sedimentary record from a small karstic lake in the Northern Levant (Yammoûneh, Lebanon): Paleoclimatic implications. Palaeogeography, Palaeoclimatology, Palaeoecology, 305, 10-27.

Dreybrodt, W., 1988. Processes in karst systems. Springer-Verlag, New York.

Dubertret, L., 1975. Introduction à la carte géologique au 1/50 000 du Liban. Notes et Mémoires du Moyen-Orient, 13, 345-403.

Edwards, R.L., Chen, J.H., Ku, T.L., & Wasserburg, G.J., 1987. Precise timing of the last interglacial period from mass-spectrometric determination of ^{230}Th in corals. Science, 236, 1547-1553.

Emeis, K.C., Schulz, H., Struck, U., Rossignol-Strick, M., Erlenkeuser, H., Howell, M.W., Kroon, D., Mackensen, A., Ishizuka, S., Oba, T., Sakamoto, T. & Koizumi, I., 2003. Eastern Mediterranean surface water temperatures and $\delta^{18}O$ during deposition of sapropels in the late Quaternary. Paleoceanography, 18, 1005, 18 p.

Fairchild, I.J., Smith, C.L., Baker, A., Fuller, L., Spötl, C., Mattey, D. & McDermott, F., 2006. Modification and preservation of environmental signals in speleothems. Earth Science Reviews, 75, 105-153.

Ford, D.C. & Williams, P.W., 2007. Karst geomorphology and hydrology. Chapman & Hall, London.

Frumkin, A., Ford, D.C. & Schwarcz, H.P., 1999. Continental oxygen isotopic record of the last 170,000 years in Jerusalem. Quaternary Research, 51, 317-327.

Frumkin, A., Ford, D.C. & Schwarcz, H., 2000. Paleoclimate and vegetation of the Last Glacial cycles in Jerusalem from a speleothem record. Global Biogeochemical Cycles, 14, 863-870.

Gasse, F., Vidal, L., Develle, A.-L. & Van Campo, E., 2011. Hydrological variability in the Northern Levant: a 250 ka multi-proxy record from the Yammoûneh (Lebanon) sedimentary sequence. Climate of the Past, 7, 1261-1284.

Gasse, F., Vidal L., Van Campo, E., Demory, F., Develle, A.-L., Tachikawa, K., Elias, A., Bard, E., Garcia, M., Sonzogni., C. & Thouveny, N., 2015. Hydroclimatic changes in northern Levant over the past 400,000 years. Quaternary Science Reviews, 111, 1-8.

Genty, D., Baker, A. & Vokal, B., 2001. Intra- and inter-annual growth rate of modern stalagmites. Chemical Geology, 176, 191-212.

Genty, D., Blamart, D., Ouahdi, R., Gilmour, M., Baker, A., Jouzel, J. & Van-Exter, S., 2003. Precise dating of Dansgaard-Oeschger climate oscillations in western Europe from stalagmite data. Nature, 421, 833-837.

Genty, D., Blamart, D., Ghaleb, B., Plagnes, V., Causse, C.h., Bakalowicz, M., Zouari, K., Chkir, N., Hellstrom, J., Wainer, K. & Bourges, F., 2006. Timing and dynamics of the last deglaciation from European and North African $\delta^{13}C$ stalagmite profiles–comparison with Chinese and South Hemisphere stalagmites. Quaternary Science Reviews, 25, 2118-2142.

Hiess, J., Condon, D.J., McLean, N. & Noble, S.R., 2012. $^{238}U/^{235}U$ systematics in terrestrial uranium-bearing minerals. Science, 335, 1610-1614.

Jaffey, A.H., Flynn, K.F., Glendenin, L.E., Bentley, W.C. & Essling, A.M.,

1971. Precision measurements of half-lives and specific activities of ^{235}U and ^{238}U. Physical Review C, 4, 1889-1906.

Kallel, N., Paterne, M., Duplessy, J.-C., Vergnaud-Grazzini, C., Pujol, C., Labeyrie, L., Arnold, M., Fontugne, M. & Pierre, C., 1997. Enhanced rainfall in the Mediterranean region during the last sapropel event. Oceanologica Acta, 20, 697-712.

Kolodny, Y., Stein, M. & Machlus, M., 2005. Sea-rain-lake relation in the Last Glacial East Mediterranean revealed by δ^{18}O- δ^{13}C in Lake Lisan aragonites. Geochimica et Cosmochimica Acta, 69, 4045-4060.

Lacave, C., Sadier, B., Delannoy, J.-J., Nehme, C. & Egozcue, J.-J., 2012. The use of speleothems to better constrain long return period seismic hazard in Lebanon. Proceedings of the 15th World Conference on Earthquake Engineering, Lisboa, Portugal. Paper no. 354.

Lisker, S., Vaks, A. & Bar-Matthews, M., 2010. Late Pleistocene palaeoclimatic and palaeoenvironmental reconstruction of the Dead Sea area (Israel), based on speleothems and cave stromatolites. Quaternary Science Reviews, 29, 1201-1211.

Lourens, L. J., Antonarakou, A., Hilgren, F. J., van Hoof, A. A. M., Vergnaud-Grazzini, C., & Zachariasse W. J., 1996. Evaluation of the Plio-Pleistocene astronomical timescale. Paleoceanography, 11, 391-413.

Nader F., 1998. The temple of speleology, Mgharet Kanaan. Al-Ouat-Ouat, 11, 54-59.

Nehme, C., Jabbour-Gedeon, B., Gerard, P.-C., Sadier, B. & Delannoy, J.J., 2009. Reconstitution sepéléogénique de la grotte de Kanaan (Antelias, Liban): contribution à la morhogenèse du Nahr Antélias. Karstologia, 54, 21-30

Nehme, C., 2013. Apport de l'endokarst dans la reconstitution des paléogéographies et environnements passés du Mont-Liban: le cas des vallées de Nahr Antelas et Nahr el-Kalb. Unpubl. Ph.D Thesis, Université de Grenoble, France.

Nehme, C., Voisin, C., Mariscal, A., Gérard, P.-C., Cornou, C., Jabbour-Gédéon, B., Amhaz, S., Salloum, N., Badaro-Saliba, N., Adjizian-Gerard, J. & Delannoy, J.J., 2013. The use of passive seismological imaging in speleogenetic studies; an example from Kanaan Cave, Lebanon. International Journal of Speleology, 42, 97-108.

Rossignol-Strick, M., 1999. The Holocene climatic optimum and pollen records of sapropel 1 in the Eastern Mediterranean, 9000–6000 BP. Quaternary Science Reviews, 18, 515-530.

Vaks, A., Bar-Matthews, M., Ayalon, A., Matthews, A., Frumkin, A., Dayan, U., Halicz, L., Almogi-Labin, A. & Schilman, B., 2006. Paleoclimate and location of the border between Mediterranean climate region and the Saharo-Arabian desert as revealed by speleothems from the northern Negev Desert, Israel. Earth and Planetary Science Letters, 249, 384-399.

Vaks, A., Bar-Matthews, M., Matthews A., Ayalon, A. & Frumkin, A., 2010. Middle-Late Quaternary paleoclimate of northern margins of the Saharan-Arabian Desert: reconstruction from speleothems of Negev Desert, Israel. Quaternary Science Reviews, 29, 2647-2662.

Verheyden, S., 2001. Speleothems as palaeoclimatic archives. Isotopic and geochemical study of the cave environment and its Late Quaternary records. Unpubl. PHD thesis. Vrije Universiteit Brussel, Belgium.

Verheyden, S., Baele, J.M., Keppens, E., Genty, D., Cattani, O., Cheng, H., Lawrence, E., Zhang, H., Van Strijdonck, M. & Quinif, Y., 2006. The Proserpine stalagmite (Han-Sur-Lesse Cave, Belgium): preliminary environmental interpretation of the last 1000 years as recorded in a layered speleothem. Geologica Belgica, 9, 245-256.

Waldmann, N., Stein, M., Ariztegui, D. & Starinsky, A., 2009. Stratigraphy, depositional environments and level reconstruction of the last interglacial Lake Samra in the Dead Sea basin. Quaternary Research, 72, 1-15.

Wang, Y.J., Cheng, H., Edwards, R.L., An, Z.S., Wu, J.Y., Shen, C.C. & Dorale, J.A., 2001. A high-resolution absolute-dated Late Pleistocene monsoon record from Hulu cave, China. Science, 294, 2345-2348.

World Bank, 2003. Republic of Lebanon: Policy note on irrigation sector sustainability. Report No. 28766– LE. The World Bank, Washington DC.

Ziegler, M., Tuenter, T. & Lourens, L.J., 2010. The precession phase of the boreal summer monsoon as viewed from the eastern Mediterranean (ODP Site 968). Quaternary Science Reviews, 29, 1481-1490.